High-Order Pulsar Timing For Navigation

Suneel I. Sheikh, *ASTER Labs, Inc.*
Ronald W. Hellings, *NASA Headquarters, Astrophysics Division*
Richard A. Matzner, *University of Texas at Austin*

BIOGRAPHY

Suneel Sheikh is Chief Research Scientist at ASTER Labs, Inc. His doctoral dissertation research investigated the use of X-ray pulsars for spacecraft navigation.

Ronald Hellings is a Research Professor at Montana State University, temporarily on assignment to NASA Headquarters as Program Scientist in the Astrophysics Division.

Richard Matzner is Professor of Physics and Director of the Center for Relativity at The University of Texas at Austin.

ABSTRACT

Proposed concepts of spacecraft navigation that utilize timing information from observational data of variable celestial sources, including pulsars, require appropriate inertial reference frames and well-defined time transfer techniques. These timing methods must be operational for any potential spacecraft position and must reach high performance to achieve accurate navigation. Algorithms that can process the signal from these sources throughout the solar system and beyond are presented here. These algorithms include the high-order relativistic effects on the propagated signal that must be incorporated to attain precise timing. A comparison is presented of existing pulsar-timing algorithms in current software codes, as well as the time-transfer algorithms defined here.

INTRODUCTION

After being theorized for many decades, spinning neutron stars were discovered in the radio band in 1967 [1]. Due to their unique periodic pulses, these neutron stars were referred to as *pulsars*. Subsequent observations have discovered pulsars emitting radiation throughout the electromagnetic spectrum [2, 3]. A particularly intriguing aspect of these celestial sources is the measured inherent stability of the periodicity of their emissions. It has been shown that their signal stability matches the quality of today's atomic clocks [4-6].

Since their discovery, accurate timing of the periodic signals from pulsars has been crucial in their observation analysis. Pulse timing is required to adequately characterize each source's unique characteristics; such as spin period, companion orbit elements, and star's evolutionary stage [2, 3]. Accurate pulse timing is also necessary for future applications that utilize these signals, such as gravitational wave detection [7-9] and spacecraft navigation [10-12].

In order to ensure accurate timing analysis of these stable sources, higher order relativistic effects must be included [2, 3, 13-16]. First-order approximations do not achieve sufficient accuracy for much of the required analysis. To investigate pulsar source characteristics, accuracies on the order of 1 μs or better are often desired. For spacecraft navigation, a desired accuracy of pulse arrival time on the order of 1 ns ($\approx$ 0.3 m) allows potentially increased position and velocity solution accuracy. Thus, any errors within the analytical timing expressions must be on the order of these uncertainties. These levels of performance also require accurate pulse timing models that predict the pulse phase over an extended time.

This paper provides an overview of the existing methods of timing the arrival of pulsar signal photons and pulses for use in today's pulsar characteristics modeling and for eventual use in spacecraft navigation applications. It also provides a method of time transfer to the center of mass of the solar system. The *Background* section provides a discussion on the methods used to model pulse time of arrivals and details on the techniques that derive the pulsar signal timing equations. The *Existing Pulsar Observation Equations* section provides a summary of the main equations in use within current analyses and operating analytical software codes. The *Barycentric Time Transfer* section identifies direct time transfer equations that could be used between any spacecraft location and the solar system center of mass, or barycenter. The *Numerical Comparisons* section provides an evaluation of the different identified algorithms based upon their simulations over various time periods. Finally some concluding remarks are provided.

BACKGROUND

Pulsar emissions can be adequately modeled due to their considerable regularity. These models are often represented as total accumulated phase. The total phase, Φ, can be modeled as the sum of the fractional portion of the pulse period, ϕ, and the total number of integer cycles, N. Thus, total phase is expressed as a function of time as,

$$\Phi(t) = \phi(t) + N(t) \tag{1}$$

Alternatively, this model may be expressed as a function of angular phase, $\Theta = 2\pi\Phi$. Based upon the characteristics of an individual pulsar, including its pulse frequency, f, and derivatives, a pulse-timing model can be created based upon total phase as,

$$\begin{aligned}\Phi(t) = \Phi(t_0) + f\left[t - t_0\right] + \frac{1}{2}\dot{f}\left[t - t_0\right]^2 \\ + \frac{1}{6}\ddot{f}\left[t - t_0\right]^3 + O\left(\dddot{f}\right)\end{aligned} \tag{2}$$

The pulse timing model of Eq. (2) is also known as the *pulsar spin equation*, or the *pulsar spin down law* [2, 3]. In this equation, the observation time, t, is the coordinate time of arrival of the signal phase, and t_0 is a chosen reference epoch for the model parameters. Higher order frequency derivatives may be required to accurately represent some pulsars, and pulsars within binary system have even further complicated pulse timing models that incorporate the pulsar orbital period [17].

The primary analysis approach for determination of pulsar characteristics, or spacecraft navigation solutions, is to compare the pulse time of arrival (TOA) measured at an observation site on Earth, or onboard an orbiting spacecraft, to the predicted arrival time based upon the model represented in Eq. (2). The TOA timing difference, or *timing residual*, is the calculated difference multiplied by the pulse period, P, as [18],

$$\delta t_{TOA} = \left\{\Phi\left(t_{TOA}\right) - \text{nint}\left[\Phi\left(t_{TOA}\right)\right]\right\} P \tag{3}$$

In Eq. (3), the function nint rounds the value to the nearest integer. In order to determine the timing residual with high performance, it is critical to compute t_{TOA} as accurately as possible, and as well as to maintain well-defined pulse-timing models.

In order to initially create accurate pulse-timing models as in Eq. (2), analytical methods must be defined that represent how to precisely time each pulse arrival. Subsequent observations utilize these same methods to accurately measure each pulse TOA. In order to reduce the complexity of these analytical methods, it is important to time the pulsar observations within an inertial reference frame that is stationary (at rest) with respect to the pulsar's frame. This requires selecting a reference frame that is appropriate for the analysis and incorporates all the necessary contributing factors that must be included for transferring pulse TOA measured in the observer's frame of reference to the selected inertial reference frame. This is done in part so that all subsequent observations can be directly compared to the model, and any effects of an observer in a rotating frame are removed. Since an observer's frame will most likely be in motion with respect to the inertial frame, as an observer on Earth or on a spacecraft in orbit, and that the observer will experience a different gravitational potential than a reference clock, the observer clock's measured *proper-time* must be converted to *coordinate time* in order to compare the result to other clocks. Standard methods provide conversions from observer's proper time to coordinate time based upon observer's clock motion and experienced gravitation potential [19-21]. These methods primarily refer to the conversion of topocentric clock observation time to coordinate time. Thus, additional considerations of different velocity and gravitational potential must be included for the spacecraft's clock circumstance [22, 23].

Once defined, the coordinate time scale and the valid location for this model must be stated in order for this model to be utilized by further observations. For many pulsar observations, the common frame utilized is the solar system barycentric (SSB) coordinate frame. This frame is referred to as the International Celestial Reference Frame (ICRF) and it axes are aligned with the equator and the equinox of epoch J2000 [24]. The reference time scale for these observations is the *Temps Coordonnée Barycentrique* (TCB, Barycentric Coordinate Time), although the slightly different time scale of the *Temps Dynamique Barycentrique* (TDB, Barycentric Dynamical Time) has also been utilized [24]. These pulse-timing models are often described to be valid at the origin of the SSB frame. In order to compare a measured pulse arrival time at a remote observation station with the predicted time at the SSB origin, the station must project arrival times of photons by its detector onto the SSB origin. This comparison requires that time be transferred from the observation station, or spacecraft, to the SSB. Alternatively, the SSB pulse-timing model could be transferred to another known location. For example, at a given time instance, the pulse timing model could be transferred to Earth's center, in order to create pulse arrival time comparisons with the position of Earth.

To accurately transfer time from one location to another, geometric and relativistic effects must be included in this transfer. These effects account for the difference in light ray paths from a source to the detector's location and to the model's location. These light ray paths can be determined using the existing theory of general relativity and the known effects of the solar system [25-27]. The equations from this theory relate the emission time of photons that emanate from a source to their arrival time at a station, and define the path of the photons traveling through curved spacetime [13-15].

Figure 1 shows the relationship of pulses from a pulsar as they arrive into the solar system relative to the SSB inertial frame and a spacecraft orbiting Earth. The positions of the spacecraft, $\mathbf{r}$, and the center of Earth, $\mathbf{r}_E$, with respect to the SSB are shown, as well as the unit direction to the pulsar, $\hat{\mathbf{n}}$. This line-of-sight vector to the pulsar can be determined relative to the SSB inertial coordinate system using its known angular location.

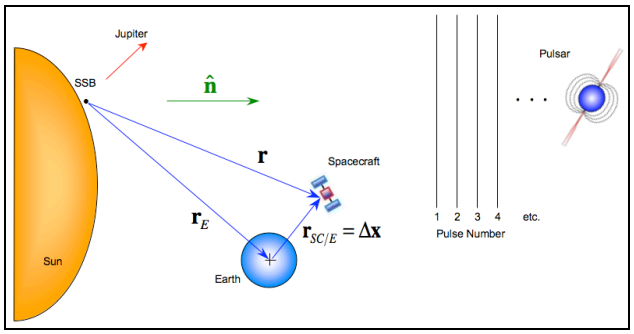

Figure 1. Spacecraft position as pulses from a distant pulsar arrive within the solar system.

A description of the pulse timing analysis approach is provided below, and follows several techniques applicable for pulsar timing analysis using Earth-based ground telescopes [13-15, 20, 21, 23, 25-27]. This description is provided here as a reference to the pulsar timing equations and the SSB time transfer equation.

An individual pulse is composed of an assemblage of photons from a pulsar within the radio, optical, and X-ray bands of the spectrum. The path taken by a photon or particle in four-dimensional spacetime is referred to as a *world line*. A *geodesic path* is the world line between two points a light ray or particle takes while in free fall within a gravitational field. For a light ray or electromagnetic signal, including those in the radio band, these paths have zero spacetime length in traveling from the emitting source to the receiving location of the observer and are referred to as *null geodesics*. Generally within a gravitational field these geodesics have some curvature in space [22, 28]. The four dimensions of the spacetime coordinate frame can be generalized to

$$\left\{x^0, x^1, x^2, x^3\right\} = \left\{ct, x, y, z\right\} \tag{4}$$

In this representation, the superscripts on the generalized coordinates, x, are indices, not exponents. The coordinate ct represents the dimension related to time with c equal to the speed of light, and $\left\{x, y, z\right\}$ represent the spatial coordinates. In the theory of general relativity, the notion of a *spacetime interval* in curved space involves the spacetime metric, $g_{\alpha\beta}$. This spacetime interval, ds, can be defined as [29],

$$ds = \sqrt{\sum_{\alpha=0}^{3}\sum_{\beta=0}^{3} g_{\alpha\beta}\, dx^{\alpha} dx^{\beta}} \tag{5}$$

The metric $g_{\alpha\beta} = g_{\alpha\beta}(ct, x, y, z)$ is a function of the time and spatial coordinates, and the elements of $g_{\alpha\beta}$ form a symmetric, covariant tensor that defines the geometry of spacetime. The dx^{α} terms are the differentials of the spacetime coordinates and define the path of an object through spacetime. The Greek indices α and β range from 0 to 3 and the Latin indices of i and j range from 1 to 3 [29]. For Minkowski's flat space of special relativity (absence of gravity), the symmetric tensor is simply the four terms of $g_{00} = -1, g_{11} = g_{22} = g_{33} = 1$, with all other terms equal to zero [28].

The spacetime interval is invariant with respect to arbitrary coordinate transformations, and its value remains constant for these transformations. The proper time, τ, measured by a clock during a pulsar observation as it moves along a world line, is related to the invariant spacetime interval and the coordinate time. From the theory of general relativity, this relationship for the spacetime interval is general with respect to the geometry of spacetime from Eq. (5) as,

$$\begin{aligned} ds^2 &= -c^2 d\tau^2 \\ &= g_{00} c^2 dt^2 + 2\sum_{j=1}^{3} g_{0j}\, c dt dx^j + \sum_{i=1}^{3}\sum_{j=1}^{3} g_{ij}\, dx^i dx^j \end{aligned} \tag{6}$$

In a weak-gravitational field and nearly flat space, which is appropriate for the solar system, a Post-Newtonian metric tensor is suitable and can be expressed to second order of the total gravitational potential within the system. Within this type of system, the spacetime interval, ds, of Eq. (6) has been shown to $O\left(1/c^4\right)$ order to be [14, 15, 27, 28],

$$\begin{aligned} ds^2 &= -c^2 d\tau^2 \\ &= -\left(1 - \frac{2U}{c^2} + \frac{2U^2}{c^4}\right) c^2 dt^2 \\ &\quad + \left(1 + \frac{2U}{c^2} + \frac{3U^2}{2c^4}\right)\left(dx^2 + dy^2 + dz^2\right) \end{aligned} \tag{7}$$

The total gravitational potential, U, acting on the spacecraft clock is the sum of the gravitational potentials of all the bodies in the solar system, and is defined in the positive sense ($U = GM\big/\sqrt{x^2 + y^2 + z^2}$ + higher order terms). Along the null geodesic paths of electromagnetic signals the spacetime interval equals zero, or $ds = 0$. Therefore the time coordinate relates to the path coordinates of Eq. (7), and using a binomial expansion this relationship is valid to order $O\left(1/c^4\right)$ as,

$$cdt = \left(1 + \frac{2U}{c^2} + \frac{7U^2}{4c^4}\right)\sqrt{dx^2 + dy^2 + dz^2} \tag{8}$$

Considering a single pulse from a source, the transmission time of each photon within the pulse is related to the reception, or observed, time of the photon by the distance

along the path this photon has traveled. Figure 2 presents a diagram of a emitting source and the observation of the photon at a spacecraft near Earth. The vector to the source from the center of the Sun is **D**, the position of the spacecraft relative to the Sun is **p**, and the line-of-sight from the spacecraft to the pulsar is $\hat{\mathbf{n}}_{SC}$. Since a pulse is an ensemble of these photons, by measuring the arrival times of all the photons within a pulse period, the arrival time of the pulse peak can be determined.

By integrating Eq. (8), an algorithm can be developed to determine when the Nth pulse is received at the spacecraft at time, t_{SC_N}, relative to when it was transmitted from the pulsar at time, t_{T_N}. This is represented as,

$$c\int_{t_{T_N}}^{t_{SC_N}} dt = \int_{D_x}^{p_x}\left(1+\frac{2U}{c^2}+\frac{7U^2}{4c^4}\right)\left[1+\left(\frac{dy}{dx}\right)^2+\left(\frac{dz}{dx}\right)^2\right]^{\frac{1}{2}} dx \quad (9)$$

In Eq. (9), p_x and D_x are the *x*-axis components of the **p** and **D** vectors of Figure 2, respectively. The solution to this equation depends on the null geodesic light ray path and the gravitational potential of bodies along this path.

Since the Sun's gravitational field is the primary field of influence within the solar system and since its field can be considered symmetric about the z-axis, a pulse of photons arriving into the solar system will travel primarily within the x-y plane as in Figure 2. Therefore, the integrated solution between a pulsar and an observation spacecraft can be computed as [14, 15, 25-27, 30],

$$\begin{aligned}\left(t_{SC_N}-t_{T_N}\right) &= \frac{1}{c}\hat{\mathbf{n}}_{SC}\cdot\left(\mathbf{D}_N-\mathbf{p}_N\right)\\ &-\sum_{k=1}^{B_{SS}}\frac{2GM_k}{c^3}\ln\left|\frac{\hat{\mathbf{n}}_{SC}\cdot\mathbf{p}_{N_k}+p_{N_k}}{\hat{\mathbf{n}}_{SC}\cdot\mathbf{D}_{N_k}+D_{N_k}}\right|\\ &+\frac{15}{4}\frac{(GM_S)^2}{c^5 D_{N_y}}\left[\arctan\left(\frac{\hat{\mathbf{n}}_{SC}\cdot\mathbf{D}_N}{D_{N_y}}\right)-\arctan\left(\frac{\hat{\mathbf{n}}_{SC}\cdot\mathbf{p}_N}{D_{N_y}}\right)\right]\\ &+\frac{2(GM_S)^2}{c^5 D_{N_y}{}^2}\left\{\begin{array}{l}\hat{\mathbf{n}}_{SC}\cdot\left(\mathbf{D}_N-\mathbf{p}_N\right)\left[\begin{array}{l}1+\left(\frac{\hat{\mathbf{n}}_{SC}\cdot\mathbf{D}_N}{D_N}\right)^2\\ -\frac{2D_{N_y}^2}{p_N D_N}\end{array}\right]\\ +2\left(\hat{\mathbf{n}}_{SC}\cdot\mathbf{D}_N\right)\left(\frac{p_N}{D_N}-1\right)\end{array}\right\}\end{aligned} \quad (10)$$

In Eq. (10), $\mathbf{p}_N$ represents position of the spacecraft when it receives the Nth pulse from the pulsar relative to the center of the Sun (not the SSB), and $\hat{\mathbf{n}}_{SC}$ is the unit direction along the path $\mathbf{D}_N$–$\mathbf{p}_N$. The first term on the right hand side of Eq. (10) is the geometric separation between the source and the observer. The second term is the summation of *Shapiro* delay effects of all the bodies within the solar system [31]. The speed of light in terms of the coordinates varies due to the strengths and positions of the gravitational potential fields along a light ray path. This effect contributes to the general relativistic effect on the transfer of time along a light ray null geodesic. The summation within this term is taken over all bodies in the solar system, B_{SS}. The terms $\mathbf{p}_{N_k}$ and $\mathbf{D}_{N_k}$ are the respective positions of the spacecraft and the source relative to the kth planetary body in the solar system at t_{SC_N} and t_{T_N}, respectively. As in Eq. (9), the subscripts *x* and *y* denote the *x*-axis and *y*-axis values of the terms from Figure 2, respectively. The third and fourth terms in this equation are the second-order effect of the deflection of the light ray path of the pulse due to the Sun, which is the primary influencing gravitational force within the solar system. These terms are typically a small value (< 40 ns) [27]. The contributions of the Sun's total angular momentum, **J**, are considered negligible here, however, may be considered for some applications [27].

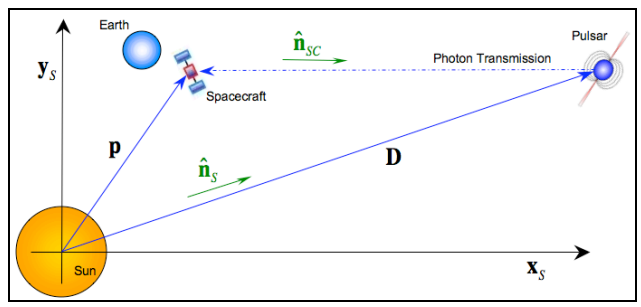

Figure 2. Light ray path arriving from distant pulsar to spacecraft within the solar system.

It is noted that Eq. (10) does not take into account all possible gravitational perturbations between a pulsar and a spacecraft detector. Many gravitational sources may exist along the photon light ray path, each affecting the total transmission time. However, since these effects are nearly constant for tens of years, for the purposes of this pulse timing analysis these effects are ignored [14, 15].

EXISTING PULSAR OBSERVATION EQUATIONS

Previous astrophysical researchers have pursued the timing analysis of pulsar signals. This section presents an overview of these previous results, as well as a discussion about the relationships of these previous algorithms to the analytical equations presented above.

Most pulsar timing implementations have utilized some form of Eq. (10) as a baseline for the algorithm used to define photon arrival times. However, modifications and simplifications have often been introduced in the implementation of this equation. There are two primary

issues with utilizing this full equation [13-15]. Firstly, the coordinate TOA, t_{SC_N}, at the spacecraft of the Nth pulse can be measured during an observation but the derivations have been done to solve for the transmission time, t_{T_N}, of the pulse from the source, in this case a pulsar. As previously mentioned, pulsar characteristics analysis should be completed in a frame at rest with respect to the pulsar, and the pulsar frame itself would be ideal for this. Thus, for characteristic analysis, a *pulsar-centric* time would be the best approach. However, the epochs for this pulsar-centric time can be many years previous to the observation date due to the vast pulsar distance, thus potentially confusing the pulse model construction and the subsequent use in future observations.

Additionally, there is the large uncertainty in the knowledge of the pulsar position, **D**. With current methods, the angular position of a pulsar can be measured to fractions of a milliarcsecond; however, its distance can only be computed in terms of fractions of a kiloparsec (1 pc ≈ 3.26 ly). For desired TOA accuracies of 1 μs or better, this uncertainty of hundred of light-years is clearly very much too large. Therefore, most algorithm simplifications primarily reconstruct a transmission time to be something attainable in the near term, and strive to remove the dependency on the pulsar distance knowledge in their implementations. The simplest method is to compare two closely sequential received pulses, effectively removing this ambiguity by differencing. Within many of these simplified timing equations, terms on order of several hundreds of nanoseconds are missing, due to these simplifications from Eq. (10).

Early representations of the pulsar timing equation, often provided without derivation, included timing relative to a topocentric clock utilized for radio telescope observations terms. An introductory equation is provided in [2] as,

$$t_b = \tau_{topo} + \frac{\hat{\mathbf{n}} \cdot \mathbf{r}}{c} - \Delta t_{DM} + \Delta t_r \tag{11}$$

In Eq. (11), t_b is the barycentric arrival time, τ_{topo} is the topocentric measurement time of the observation, and **r** is the position of the measurement clock with respect to the SSB. This second term represents a simple geometric displacement of the clock from the SSB. The third term is due to the interstellar plasma (medium) delay, and is equal to

$$\Delta t_{DM} = \frac{(0.00415)DM}{f^2} \tag{12}$$

where DM is the column density of electrons, or the dispersion measure, in units of pc/cm^3, and f is the observing frequency in GHz. This term is significant only for radio and optical observation frequencies, as the X-ray spectrum is near "infinite" frequency, thus this term is considered negligible for X-ray observations. The final term in this equation, Δt_r, is relativistic clock correction of clock on Earth's surface [2].

An updated form of this timing equation is provided in [32] as,

$$t_b = \tau_{topo} + \frac{|\mathbf{D} - \mathbf{r}|}{c} - \Delta t_{DM} + \Delta t_{E\odot} \tag{13}$$

This form of the equation introduces the transmission time from the source in the second term. However, as noted in the reference, the second term is expanded with respect to the ratio of distance magnitudes *r/D*, which to first order is equals the second term of Eq. (11), once the leading term equivalent to the total pulsar distance, *D*, is absorbed into the representation of the initial epoch of phase [32]. The term $\Delta t_{E\odot}$ is the solar system's Einstein delay, which is a combined effect of gravitational redshift of Earth and other bodies and time dilation due to the motion of Earth, and can be expressed as an integral [32],

$$\frac{d\Delta_{E\odot}}{dt} = \sum_{k=1}^{B_{SS}} \frac{GM_k}{c^2 r_k} + \frac{\upsilon_E^2}{2c^2} - \text{constant} \tag{14}$$

In Eq. (14), M_k is the mass of each solar system body other than Earth, and r_k is the distance of body k from Earth, and υ_E is Earth speed with respect to the SSB.

An additional representation of the timing equation includes added relativistic effects as [33],

$$t_b = \tau_{topo} + \frac{\hat{\mathbf{n}} \cdot \mathbf{r}}{c} - \Delta t_{DM} + \Delta t_{E\odot} - \Delta t_{S\odot} \tag{15}$$

The final term of Eq. (15) is the Shapiro delay term, and is expressed as [33],

$$\Delta t_{S\odot} = -\frac{2GM_S}{c^3} \ln\left(1 + \cos\theta\right) \tag{16}$$

In Eq. (16), θ is the pulsar-Sun-Earth angle at the time of the observation.

Further representations including the topocentric observation time expand the second term of Eq. (13) to include second order effects as [5, 34, 35],

$$t_b = \tau_{topo} + \frac{\hat{\mathbf{n}} \cdot \mathbf{r}}{c} + \frac{(\hat{\mathbf{n}} \cdot \mathbf{r})^2 - r^2}{2cD} - \Delta t_{DM} + \Delta t_{E\odot} - \Delta t_{S\odot} + \Delta t_{A\odot} \tag{17}$$

In Eq. (17), $\Delta t_{A\odot}$ is aberration delay due to Earth's rotation [33, 34]. The various representations from Eqs. (11), (13), (15), and (17) provide pulsar timing equations that transform the topocentric observation time to the barycentric coordinate time. From these observations, the characteristics of the pulsar itself can be investigated.

The derivation documented in [13] provides additional insight to the methods of pulsar timing. Derived from the relativistic path equations, it relates a coordinate time of observation (assuming the proper time has already been

converted to the appropriate coordinate time scale), t_{SC}, to a barycentric observation time as,

$$t_b = t_{SC} + \frac{\hat{\mathbf{n}}\cdot\mathbf{r}}{c} - \frac{1}{2cD}\left\|\hat{\mathbf{n}}\times\mathbf{r}\right\|^2 + \frac{2GM_S}{c^3}\left[\frac{1}{2}\left(1-\hat{\mathbf{n}}\cdot\mathbf{r}\right) - \ln\left|\frac{2D}{r\left(1+\hat{\mathbf{n}}\cdot\mathbf{r}\right)}\right|\right] \tag{18}$$

The statements are made clear in the text that this Eq. (18) provides a barycentric date of the observation, and is not the same as the time of arrival at the barycenter of a photon emitted from a source [13].

Another detailed derivation of the pulsar signal timing analysis is provided in [14, 15], which builds upon the relativistic work accomplished in [25-27, 30]. This analysis presents several simplifications to the full Eq. (10) in order to address the implementation issues of this equation as cited above. The initial simplification recommends that for 100 ns accuracy it is only necessary to consider the first two terms of the Eq. (10) such that,

$$t_{T_N} = t_{SC_N} - \frac{1}{c}\left\|\mathbf{D}_N - \mathbf{p}_N\right\| + \sum_{k=1}^{B_{SS}} \frac{2GM_k}{c^3}\ln\left|\frac{\hat{\mathbf{n}}_{SC}\cdot\mathbf{p}_{N_k} + p_{N_k}}{\hat{\mathbf{n}}_{SC}\cdot\mathbf{D}_{N_k} + D_{N_k}}\right| \tag{19}$$

In Eq. (19), the first term from Eq. (10) has been rearranged in terms of path magnitude. However, this resulting equation still includes the largely ambiguous pulsar position term, **D**. Thus, further modification includes the knowledge of the change in position of the pulsar. The proper-motion of the emitting source can be included for the change of the pulsar's location from its position, $\mathbf{D}_0$, at the emission of the 0th pulse at t_{T_0}, and its position, $\mathbf{D}_N$, of the Nth pulse at t_{T_N} [14]. Assuming a constant proper motion, $\mathbf{V}$, and that the difference in transmission time is considered equal to the difference in reception time, such that $\Delta t_N \equiv (t_{T_N} - t_{T_0}) \cong (t_{SC_N} - t_{SC_0})$, the pulsar position can be represented as,

$$\mathbf{D}_N = \mathbf{D}_0 + \mathbf{V}\Delta t_N \tag{20}$$

The line-of-sight can be represented from Eq. (20) as $\hat{\mathbf{n}}_N = \mathbf{D}_N / D_N$, and its initial value as $\hat{\mathbf{n}}_0 = \mathbf{D}_0 / D_0$. If the line-of-sight to the emitting source is considered constant within the solar system, then the separate directions become $\hat{\mathbf{n}}_{SC} \approx \hat{\mathbf{n}}_{SSB} \approx \hat{\mathbf{n}}_S \approx \hat{\mathbf{n}}_N$.

The significant modification recommended in [14, 15] involves a change in origin within the equation from a Sun centered frame to the SSB frame. The assumption is that the subtraction of a constant offset does not affect the final pulsar timing analysis since any fixed value can be absorbed into the initial phase epoch. Therefore, in the first term of Eq. (19), the heliocentric position of the clock, **p**, can be replaced by the barycentric position, **r**, resulting in the following using Eq. (20),

$$t_{T_N} = t_{SC_N} - \frac{1}{c}\left\|(\mathbf{D}_0 + \mathbf{V}\Delta t_N) - \mathbf{r}_N\right\| + \sum_{k=1}^{B_{SS}} \frac{2GM_k}{c^3}\ln\left|\frac{\hat{\mathbf{n}}_N\cdot\mathbf{p}_{N_k} + p_{N_k}}{\hat{\mathbf{n}}_N\cdot\mathbf{D}_{N_k} + D_{N_k}}\right| \tag{21}$$

Figure 3 presents a diagram of the positions of the pulsar, the spacecraft, and the SSB with respect to the Sun.

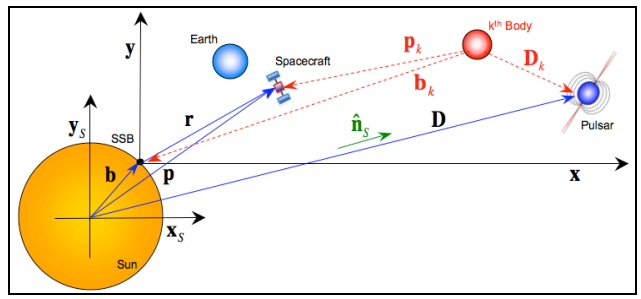

Figure 3. Spacecraft position relative to Sun, SSB origin, and other planetary bodies.

Eq. (21) retains the full position of the pulsar, $\mathbf{D}$, as well as the transmission time, t_{T_N}. Since these cannot be determined to the accuracy required by the pulsar timing analysis or are unknown, a new term is introduced to the algorithm in order to gather these unknown terms into values that can be effectively ignored within pulsar timing analysis. This is due to the selection of the initial epoch as an arbitrary value. Also, since the timing residual difference of Eq. (3) is a relative difference, a fixed offset in the computation of Φ(TOA) does not affect the residual computation (only the absolute value of Φ is effected). Thus, the introduction of a zero-order TOA into the solar system is introduced as,

$$t_{SC_0} = t_{T_0} + \frac{D_0}{c} - \sum_{k=1}^{B_{SS}} \frac{2GM_k}{c^3}\ln\left|\frac{1}{\hat{\mathbf{n}}_N\cdot\mathbf{D}_{N_k} + D_{N_k}}\right| \tag{22}$$

Subtracting this fixed value from Eq. (21) along with the above simplifications results in a simplified expression of,

$$\begin{aligned}\left(t_{T_N} - t_{T_0}\right) &= \left(t_{SC_N} - t_{SC_0}\right) + \frac{1}{c}\left[\left(\hat{\mathbf{n}}_0\cdot\mathbf{r}_N\right) - \left(\hat{\mathbf{n}}_0\cdot\mathbf{V}\Delta t_N\right)\right] \\ &+ \frac{1}{2cD_0}\left[\left(\hat{\mathbf{n}}_0\cdot\mathbf{r}_N\right)^2 - r_N^2\right] \\ &- \frac{1}{cD_0}\left[\left(\hat{\mathbf{n}}_0\cdot\mathbf{V}\right)\left(\hat{\mathbf{n}}_0\cdot\mathbf{r}_N\right) - \left(\mathbf{V}\cdot\mathbf{r}_N\right)\right]\Delta t_N \\ &+ \frac{1}{2cD_0}\left[\left(\hat{\mathbf{n}}_0\cdot\mathbf{V}\right)^2 - V^2\right]\Delta t_N^2 \\ &+ \sum_{k=1}^{B_{SS}} \frac{2GM_k}{c^3}\ln\left|\hat{\mathbf{n}}_N\cdot\mathbf{p}_{N_k} + p_{N_k}\right|\end{aligned} \tag{23}$$

This equation does not solve for the pulse arrival time at the SSB (as incorrectly portrayed in many papers). Rather

it provides a *pulsar-centric* difference time ($t_{T_N} - t_{T_0}$) against which a given observation ($t_{SC_N} - t_{SC_0}$) can be compared. However, it is easy to see how this is misunderstood, as seen by the representations in several of the existing equations. Implementations of these equations have incorrectly referred to this correction as a *bary-centering* process, since ignoring the zeroth order term t_0 makes the equations appear to transfer time from the observer's position to the barycenter origin. The actual true concept is *pulsar-centerin*g of the photon into a frame origin that is at rest with respect to the pulsar. As discussed in [14, 15], the left-hand side of Eq. (23) involves the model of the rotation dynamics of the pulsar. The second term on the right-hand side is the first-order Doppler delay. The third term is due to the effects of annual parallax, and together with the second term is *Roemer* delay. The forth term, proportional to Δt_N, is due to the pulsar's proper motion. The fifth term, proportional to Δt_N^2 is due to the pulsar's transverse motion. The sixth term is the Shapiro delay effect.

Discussions have been presented regarding the timing of pulsars within binary systems [17, 36, 37]. Binary system pulsars have additional complexity within their timing models, as well as considerations of the additional relativistic effects produced by the companion star's mass. The Shapiro delay terms in these systems can be represented similarly as the isolated pulsar sources. However these papers present considerations of only the time-varying portion of the Shapiro delay effects, and do not create a time difference between the pulse arrival at Earth-based telescopes and the SSB.

Both these relativistic-based analyses of [13] and [14, 15] assume the coordinate arrival time of a photon at the observation station on Earth. They could be applicable to spacecraft if the spacecraft's position is substituted for Earth position, although the added effects of a spacecraft's motion and gravitational potential must be included when converting from proper-time to coordinate time. The position of the Sun, planetary bodies, and observer's position, **p**, can be well known (to tens of meters) to allow accurate knowledge of these terms within this timing equation for pulsar characteristic observations.

BARYCENTRIC TIME TRANSFER

This section presents a method of specific time transfer between an arbitrary solar system position and the SSB. Although it does not exactly match existing pulsar barycentric date of observation calculations, it can be used for applications of direct time transfer.

In order to make a direct comparison of the pulse arrival time at the spacecraft relative to its projected arrival time at the SSB, time must be transferred from the spacecraft to the SSB. This time transfer can be accomplished by differencing the transmit time of the Nth pulse from a pulsar, t_{T_N}, to its arrival at each of the spacecraft, t_{SC_N}, and the SSB, t_{SSB_N}, as in

$$\left(t_{SSB_N} - t_{T_N}\right) - \left(t_{SC_N} - t_{T_N}\right) = t_{SSB_N} - t_{SC_N} \tag{24}$$

Eq. (10) provides the time difference from the transmission source to the spacecraft, ($t_{SC_N} - t_{T_N}$), which is based upon the heliocentric spacecraft position of **p**. A similar representation of Eq. (10) can be made for the true SSB position, **b**, as shown in Figure 3 (the interested reader is referred to Eq. 4.26 of [11] for the expression). Substituting this new expression into Eq. (24), the direct difference yields the necessary transfer time between the spacecraft and the SSB as,

$$\begin{aligned}
\left(t_{SSB} - t_{SC}\right) &= \frac{1}{c}\left[\left(\hat{\mathbf{n}}_{SC}\cdot\mathbf{p}\right) - \left(\hat{\mathbf{n}}_{SSB}\cdot\mathbf{b}\right)\right] + \frac{1}{c}\left(\hat{\mathbf{n}}_{SSB} - \hat{\mathbf{n}}_{SC}\right)\cdot\mathbf{D} \\
&+ \sum_{k=1}^{B_{SS}} \frac{2GM_k}{c^3} \ln\left|\left(\frac{\hat{\mathbf{n}}_{SC}\cdot\mathbf{p}_k + p_k}{\hat{\mathbf{n}}_{SSB}\cdot\mathbf{b}_k + b_k}\right)\left(\frac{\hat{\mathbf{n}}_{SSB}\cdot\mathbf{D}_k + D_k}{\hat{\mathbf{n}}_{SC}\cdot\mathbf{D}_k + D_k}\right)\right| \\
&+ \frac{2(GM_S)^2}{c^5 D_{y_{SSB}}^2}\left\{\begin{array}{l}
\hat{\mathbf{n}}_{SSB}\cdot\left(\mathbf{D}-\mathbf{b}\right)\left[1+\left(\frac{\hat{\mathbf{n}}_{SSB}\cdot\mathbf{D}}{D}\right)^2 - 2\frac{D_{y_{SSB}}^2}{bD}\right] \\
+2\left(\hat{\mathbf{n}}_{SSB}\cdot\mathbf{D}\right)\left(\frac{b}{D}-1\right) \\
+\frac{15}{8}D_{y_{SSB}}\left[\begin{array}{l}\arctan\left(\frac{\hat{\mathbf{n}}_{SSB}\cdot\mathbf{D}}{D_{y_{SSB}}}\right) \\ -\arctan\left(\frac{\hat{\mathbf{n}}_{SSB}\cdot\mathbf{b}}{D_{y_{SSB}}}\right)\end{array}\right]
\end{array}\right\} \\
&- \frac{2(GM_S)^2}{c^5 D_{y_S}^{\ 2}}\left\{\begin{array}{l}
\hat{\mathbf{n}}_{SC}\cdot\left(\mathbf{D}-\mathbf{p}\right)\left[1+\left(\frac{\hat{\mathbf{n}}_{SC}\cdot\mathbf{D}}{D}\right)^2 - 2\frac{D_{y_S}^2}{pD}\right] \\
+2\left(\hat{\mathbf{n}}_{SC}\cdot\mathbf{D}\right)\left[\frac{p}{D}-1\right] \\
+\frac{15}{8}D_{y_S}\left[\begin{array}{l}\arctan\left(\frac{\hat{\mathbf{n}}_{SC}\cdot\mathbf{D}}{D_{y_S}}\right) \\ -\arctan\left(\frac{\hat{\mathbf{n}}_{SC}\cdot\mathbf{p}}{D_{y_S}}\right)\end{array}\right]
\end{array}\right\}
\end{aligned} \tag{25}$$

In Eq. (25), the subscript for the Nth pulse received at each location has been dropped for clarity, and several terms have been rearranged for improved numerical characteristics. The resulting equation is the full second-order high accuracy time transfer equation between the spacecraft and the SSB, and should be accurate to sub-nanosecond if all terms are retained.

Since Eq. (25) still includes the ambiguous source position **D**, the arguments for simplification as presented above due to the pulsar position and line of sight can be directly followed. Neglecting the difference of the third and fourth terms should have small effect, since the difference of these two small values can be effectively ignored. When the position of the spacecraft relative to the SSB, $\mathbf{r}$ (such that $\mathbf{p} = \mathbf{b} + \mathbf{r}$), is used, then these simplifications modify the time transfer equation to relate t_{SC} and t_{SSB}, to the following,

$$\left(t_{SSB} - t_{SC}\right) = \frac{1}{c}\left[\begin{array}{l} \hat{\mathbf{n}}_0 \cdot \mathbf{r} - \dfrac{r^2}{2D_0} + \dfrac{\left(\hat{\mathbf{n}}_0 \cdot \mathbf{r}\right)^2}{2D_0} + \dfrac{\mathbf{r} \cdot \mathbf{V}\Delta t_N}{D_0} \\ - \dfrac{\left(\hat{\mathbf{n}}_0 \cdot \mathbf{V}\Delta t_N\right)\left(\hat{\mathbf{n}}_0 \cdot \mathbf{r}\right)}{D_0} \\ + \dfrac{\left(\hat{\mathbf{n}}_0 \cdot \mathbf{r}\right)}{D_0^2}\left[\left(\mathbf{r} \cdot \mathbf{V}\Delta t_N\right) - \dfrac{r^2}{2}\right] \\ + \dfrac{\left(\hat{\mathbf{n}}_0 \cdot \mathbf{V}\Delta t_N\right)}{D_0^2}\left[\dfrac{r^2}{2} - \left(\mathbf{r} \cdot \mathbf{V}\Delta t_N\right)\right] \\ - \dfrac{\left(\mathbf{b} \cdot \mathbf{r}\right)}{D_0} + \dfrac{\left(\hat{\mathbf{n}}_0 \cdot \mathbf{b}\right)\left(\hat{\mathbf{n}}_0 \cdot \mathbf{r}\right)}{D_0} \\ + \dfrac{\left(\hat{\mathbf{n}}_0 \cdot \mathbf{r}\right)}{D_0^2}\left[-\left(\mathbf{b} \cdot \mathbf{r}\right) - \dfrac{b^2}{2} + \left(\mathbf{b} \cdot \mathbf{V}\Delta t_N\right)\right] \\ + \dfrac{\left(\hat{\mathbf{n}}_0 \cdot \mathbf{b}\right)}{D_0^2}\left[-\left(\mathbf{b} \cdot \mathbf{r}\right) - \dfrac{r^2}{2} + \left(\mathbf{r} \cdot \mathbf{V}\Delta t_N\right)\right] \\ + \dfrac{\left(\hat{\mathbf{n}}_0 \cdot \mathbf{V}\Delta t_N\right)\left(\mathbf{b} \cdot \mathbf{r}\right)}{D_0^2} \end{array}\right] + \sum_{k=1}^{B_{SS}} \frac{2GM_k}{c^3} \ln\left|\frac{\hat{\mathbf{n}}_N \cdot \mathbf{p}_k + p_k}{\hat{\mathbf{n}}_N \cdot \mathbf{b}_k + b_k}\right| \tag{26}$$

Ignoring all terms of order $O\left(1/D_0^2\right)$ yields a time transfer algorithm of,

$$\left(t_{SSB} - t_{SC}\right) = \frac{1}{c}\left[\begin{array}{l} \hat{\mathbf{n}}_0 \cdot \mathbf{r} - \dfrac{r^2}{2D_0} + \dfrac{\left(\hat{\mathbf{n}}_0 \cdot \mathbf{r}\right)^2}{2D_0} + \dfrac{\mathbf{r} \cdot \mathbf{V}\Delta t_N}{D_0} \\ - \dfrac{\left(\hat{\mathbf{n}}_0 \cdot \mathbf{V}\Delta t_N\right)\left(\hat{\mathbf{n}}_0 \cdot \mathbf{r}\right)}{D_0} \\ - \dfrac{\left(\mathbf{b} \cdot \mathbf{r}\right)}{D_0} + \dfrac{\left(\hat{\mathbf{n}}_0 \cdot \mathbf{b}\right)\left(\hat{\mathbf{n}}_0 \cdot \mathbf{r}\right)}{D_0} \end{array}\right] + \sum_{k=1}^{B_{SS}} \frac{2GM_k}{c^3} \ln\left|\frac{\hat{\mathbf{n}}_N \cdot \mathbf{p}_k + p_k}{\hat{\mathbf{n}}_N \cdot \mathbf{b}_k + b_k}\right| \tag{27}$$

Since the Sun imposes the primary gravitational field within the solar system, the expression in Eq. (27) may be further simplified as,

$$\left(t_{SSB} - t_{SC}\right) = \frac{\hat{\mathbf{n}}_0 \cdot \mathbf{r}}{c} + \frac{1}{2cD_0}\left[\begin{array}{l} \left(\hat{\mathbf{n}}_0 \cdot \mathbf{r}\right)^2 - r^2 + 2\mathbf{r} \cdot \mathbf{V}\Delta t_N \\ -2\left(\hat{\mathbf{n}}_0 \cdot \mathbf{V}\Delta t_N\right)\left(\hat{\mathbf{n}}_0 \cdot \mathbf{r}\right) \\ +2\left(\hat{\mathbf{n}}_0 \cdot \mathbf{b}\right)\left(\hat{\mathbf{n}}_0 \cdot \mathbf{r}\right) - 2\left(\mathbf{b} \cdot \mathbf{r}\right) \end{array}\right] + \frac{2GM_S}{c^3} \ln\left|\frac{\hat{\mathbf{n}}_N \cdot \mathbf{p} + p}{\hat{\mathbf{n}}_N \cdot \mathbf{b} + b}\right| \tag{28}$$

Since pulse timing models could be defined at any known location, such as Earth–center, Earth–Moon barycenter, Mars–center, even other spacecraft locations, it may be necessary to implement time transfer to locations other than the SSB. These equations can be used to transfer time between the spacecraft and another reference position, by replacing the position of the SSB's origin, $\mathbf{b}$, with the new reference position (ex. $\mathbf{r}_E$, if the model is defined at Earth–center). Thus, these expressions provide a method to accurately compare the pulse arrival time at the spacecraft with those of pulsar timing models that can be defined at any known location within the solar system.

Time transfer will be an important aspect for accurate spacecraft navigation using pulsars. However, as can be seen in these equations, this time transfer requires knowledge, or an estimate, of detector position in order to be implemented. It has been shown that this dilemma can still be addressed in order to determine spacecraft position and velocity [11, 12, 38].

NUMERICAL COMPARISONS

Shapiro Delay Expressions

It is noted in the various pulsar timing equations of (11), (13), (15), (17), (18), and (23) that there are many similarities in the Doppler and Roemer delay terms, aside from some assumptions such as constant source position. However, this is not necessarily true of the listed Shapiro delay terms. Due to their derivations, or underlying assumptions, several of these equations have unique expressions for this effect. Although this term is a secondary effect, it still amounts to hundreds of microseconds, so it is important to properly evaluate this term correctly for improved accuracy.

Several valuable software codes have been written to provide researchers with analysis tools for investigating these sources. These include the pulsar timing code TEMPO [18], and the X-ray photon processing code AxBary [39]. A comparison of the expressions used for Shapiro delay in these software codes versus those proposed by the cited references is provided below.

Designed specifically for pulsar timing and characteristic analysis, the TEMPO code provides a significant tool for astrophysics research. Developed primarily at Princeton

University, this code largely follows the equations from [14, 15, 32, 33] for topocentric radiometric observations, although some provisions are provided for spacecraft based measurements. In its later code versions, most of the pulsar timing equation of Eq. (23) is included, however, the implemented Shapiro delay term is computed as,

$$\Delta t_{S\odot} = -\frac{2GM_S}{c^3}\ln\left|\frac{p}{AU}\left(1+\cos\theta\right)\right| \tag{29}$$

The cosine term is specifically implemented as,

$$\cos\theta = \left(\hat{\mathbf{n}}_N \cdot \hat{\mathbf{p}}\right) \tag{30}$$

Designed as a software processing tool to generate pulse TOAs from direct X-ray astronomy observations, AxBary is a component of an analysis software package, provided in part by the NASA HEASARC facility [39, 40]. Its implementation within the software file bary.c of Shapiro delay is the same as Eq. (16), which is similar to Eq. (29) without the extra scaling factor.

Since the expression of Shapiro delay in Eq. (23) is the result after the zero-order TOA term of Eq. (22) is removed, it contains units of the position variables within the logarithm term. Although this expression provides the additional contributions of all planetary bodies, some scaling factor must be included to insure the argument of the logarithmic term is unitless. To provide a comparison to the remaining equations in this analysis, the logarithmic arguments were scaled by dividing by 1 AU.

Two representative pulsars and their known parameters were selected to complete the comparison process. These were the Crab pulsar (PSR B0531+21) and PSR B1937+21. The ephemeris data from each source was provided from observational archives. For PSR B0531+21, a position of RA = $05^h34^m31^s.973$, Dec = +22°00′52″.06, distance = 2 kpc, a proper motion of μ_α = -17 mas/yr and μ_δ = 7 mas/yr at epoch 48743.0 MJD [41-44]. For PSR B1937+21 a position of RA = $19^h39^m38^s.5600084$, Dec = +21°34′59″.13548, distance = 3.6 kpc, a proper motion of μ_α = -0.128 mas/yr and μ_δ = -0.486 mas/yr at epoch 52328.0 MJD [41, 45].

A simulation was created to evaluate these comparisons. To incorporate the known positions of the solar system bodies, the JPL DE405 ephemeris tables were utilized [46]. It was assumed that all times within the simulation were coordinate observation times, thus no proper time conversion was implemented. To simulate the position of a spacecraft observing the chosen pulsars, a position at conjunction of Earth with respect to the Sun was chosen, effectively placing the spacecraft on the opposite side of the Sun in Earth's orbit (selected as a 182 day lag behind Earth).

Evaluations were completed for each pulsar over two years, starting from 1 January 2006, and 25 years from this same epoch used to represent two periods of Jupiter's orbit, the second most dominant gravitational effect within the Shapiro delay equations. Plots of the differences of each expression from the TEMPO version of Eq. (29) were created. To show the comparison sufficiently, these plots have the initial difference offset (if any) from each set removed. This removal of the constant offset is a valid assessment since the zeroth order phase epoch is arbitrary.

The Shapiro delay expression for three pulsar timing methods is differenced with respect to the delay from TEMPO for PSR B1937+21 is shown in Figure 4. This comparison is plotted over two years to show the cyclic effects within the graphs. The difference between TEMPO and AxBary is periodic due to the inclusion of the spacecraft position in Eq. (29) as opposed to Eq. (16). The amplitude of this difference during this time frame reaches 330 ns. The amplitude of the difference using Eq. (18) reaches 60 ns, whereas for Eq. (23) the amplitude only reaches 36 ns. Due to the changing position of the major planets, including Jupiter, over 25 years the differences for Eq. (18) reaches 125 ns and for Eq. (23) reaches 55 ns.

For the Crab pulsar, the Shapiro delay difference plots over two years are shown in Figure 5. Although the same cyclic effects are visible in the plots of the AxBary difference with a magnitude reaching 330 ns, the plots show some numerical instability for the differences of Eqs. (18) and (23). This is caused by the instability of the logarithm term as the line of sight to the pulsar from the spacecraft intersects with the Sun. If the regions where the logarithm is unstable are removed, since it is likely the pulsar could not be observed during these times due to the Sun, then the difference over 25 years of Eq. (18) reaches values on the order of 500 ns and Eq. (23) reaches 50 ns.

For future use of these timing equations, it is important to note their potential numerical uncertainties in all terms, including the Shapiro delay expression. To address some of this uncertainty, a recently developed software code has been made available to the public. This next generation of pulsar timing code, named TEMPO2, attempts to increase the level of performance of timing of these sources [47, 48]. Some unique attributes of this code include the use of the TCB time scale, quadruple precision data processing, and the inclusion of additional planets to the Shapiro delay computation. With a stated accuracy of 1 ns or better, future analysis is planned to compare TEMPO2's defined timing equation with those discussed here.

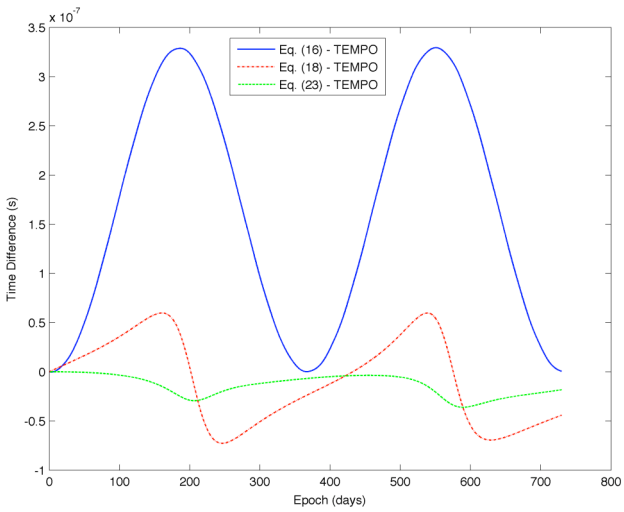

Figure 4. Differences of Shapiro delay magnitude for PSR B1937+21. Initial offset from each difference has been removed for clarity. The initial epoch is 1 January 2006.

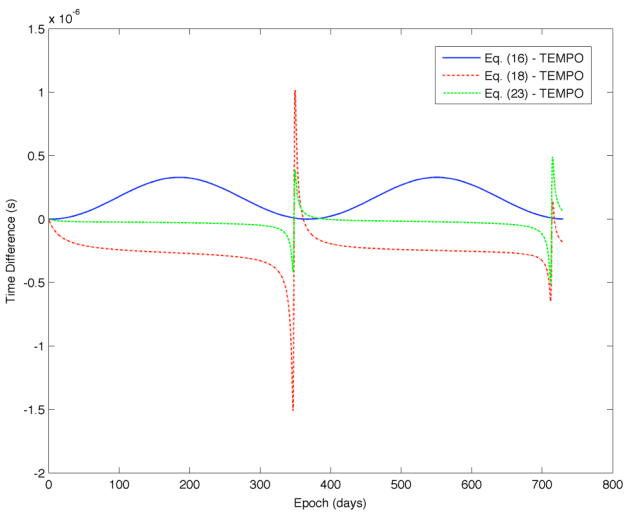

Figure 5. Differences of Shapiro delay magnitude for the Crab pulsar, with initial difference offset removed. Initial epoch is 1 January 2006.

SSB Time Transfer Expressions

The equations of time transfer in the solar system of Eqs. (25), (26), (27), and (28) provide decreasing complexity of computation, however, these also produce diminishing accuracy. Depending on the performance required by a specific application, the algorithm with adequate accuracy should be utilized. Therefore, a simulation of these equations was created to evaluate their performance over two and 25 years. This was a similar set up as the Shapiro delay simulation, with all times being coordinate times, the JPL DE405 ephemeris used for solar system object positions, and the same pulsars being analyzed.

In order to produce the results of the simulation it was required to utilize *variable precision arithmetic* to compute the differences between large and small values. This was implemented to avoid the potential numerical truncation, which ignores small remainders, when using fixed double precision. It is recommended that quadruple precision (128 bits of floating point) be used if any of the Eqs. (25)–(28) are implemented for deep space missions.

The plot of Figure 6 provides the differences for the simplified SSB time transfer equations with respect to Eq. (25) over a two-year duration. The differences for Eqs. (26) and (27) are nearly the same (thus the line graphs lie nearly on top of each other in this figure) with a maximum difference of 65 ps during this time frame and a maximum of 780 ps over the 25 years. The simplification of considering only the Sun's Shapiro delay effect causes the difference for Eq. (28) to reach 3 ns over full 25 years duration. The plot of Figure 7 shows the time transfer differences for the Crab pulsar over the same time duration. Due to the line of sight to the pulsar approaching the Sun towards the end of the first year and more pronounced in the second year, the logarithm terms can grow unbounded, therefore the plot is windowed for clearer view of the differences outside this region. If this unbounded region is ignored, the differences for Eqs. (26) and (27) reach approximately 2 ns over 25 years, and the difference for Eq. (28) reaches 5 ns. Using any of the simplified expressions from Eq. (26), (27), or (28) provides a method to transfer time from the spacecraft's position to the SSB position. When using one of these equations to operate within a navigation system, it is important to consider reference time scales, pulsar phase timing model definitions, and desired accuracy in order to insure correct time transfer results.

Although they were designed primarily for Earth based observations, it is interesting to note the effects on the pulse timing equations at various possible spacecraft locations throughout the solar system. If a spacecraft were hypothetically at the center of the Sun (approximated as a point mass) and assuming negligible effects from other planetary bodies, then within Eq. (10) $\mathbf{p} = \mathbf{0}$ and the Shapiro delay is infinite, which can be discarded as a constant in a pulsar timing analysis, leaving primarily only the fixed geometric delay term. However, if a spacecraft were at the SSB such that $\mathbf{p} = \mathbf{b}$, then the Shapiro delay term continues to have cyclic effects due to the motion of the Sun about the barycenter. The derived equations of Eqs. (25) through (28) describe the transfer of time from a spacecraft to the SSB. Therefore, when a spacecraft is hypothetically at the SSB where $\mathbf{r} = \mathbf{0}$ (and $\mathbf{p} = \mathbf{b}$) all equations compute a zero time difference. This includes the Shapiro delay term for these equations. In contrast to the pulsar timing equations, these time transfer equations would have cyclic effects if a spacecraft is located at the Sun's center ($\mathbf{p} = \mathbf{0}$), assuming the infinite Shapiro delay effect is discarded. The fundamental difference is that pulsar timing analysis equations

determine the barycentric photon arrival time with respect to the pulsar by removing the unknown transmission time, whereas the time transfer equations project the measured photon arrival time at a known position to the SSB origin.

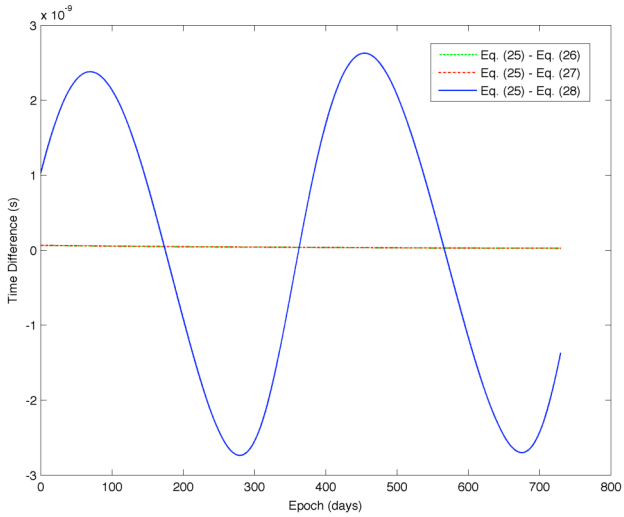

Figure 6. Differences of SSB time transfer equations for PSR B1937+21. Initial epoch is 1 January 2006.

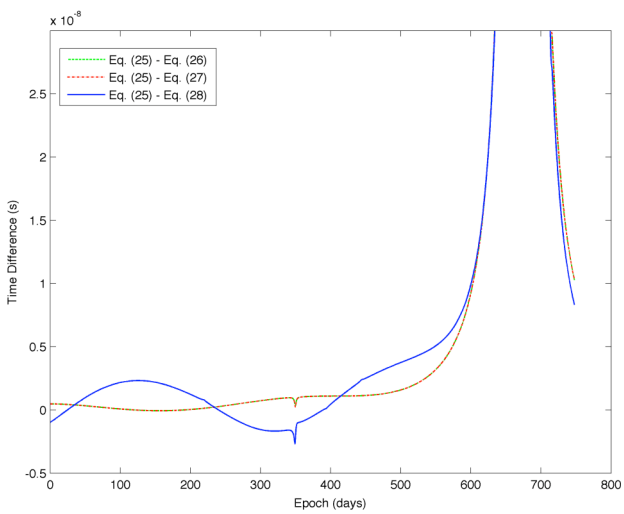

Figure 7. Differences of SSB time transfer equations for Crab pulsar. Initial epoch is 1 January 2006.

CONCLUSIONS

Accurately timing pulses from pulsars is important for astrophysics research and applications such as spacecraft navigation. As the state of the art advances in these fields, timing algorithms that provide nanosecond level accuracy are being pursued. Currently utilized methods have errors on the order of hundreds of nanoseconds based upon their implementation simplifications, which should be addressed if improved accuracies are required. A time transfer equation within the solar system is provided here based upon the same pulse-timing derivation techniques, with simplified forms expected to be accurate to tens of nanoseconds or less. Further research plans include considering derivations that are not restricted to a straight line photon light-ray path, investigating the implications of neglecting the Sun's total angular momentum, reviewing additional components for binary star systems, and studying the newer implementations within the latest analysis software codes.

ACKNOWLEDGMENTS

We acknowledge the contributions of Paul Ray, Kent Wood, and Michael Wolff and of the Naval Research Laboratory for their helpful discussions on pulsar timing. We thank David Nice, formerly of Princeton University, for his generous discussion on the timing within the TEMPO code. We also recognize the many helpful related pulsar-based navigation discussions from the DARPA XNAV team members, especially Neil Ashby. Much of this research was supported by the fellowship program of the Metropolitan Washington DC Chapter of the Achievement Rewards for College Scientists (ARCS) Foundation and the Gustave J. Hokenson Fellowship of the Aerospace Engineering Department of the University of Maryland. R.M. acknowledges support from NSF PHY0354842, and NASA grant NNG04GL37G.

REFERENCES

[1] Hewish, A., Bell, S. J., Pilkington, J. D., Scott, P. F., and Collins, R. A., "Observation of a Rapidly Pulsating Radio Source," *Nature*, Vol. 217, 1968, pp. 709-713.

[2] Manchester, R. N., and Taylor, J. H., *Pulsars*, W.H. Freeman and Company, San Francisco CA, 1977.

[3] Lyne, A. G., and Graham-Smith, F., *Pulsar Astronomy*, Cambridge University Press, Cambridge UK, 1998.

[4] Taylor, J. H., "Millisecond Pulsars: Nature's Most Stable Clocks," *Proceedings of the IEEE*, Vol. 79, No. 7, 1991, pp. 1054-1062.

[5] Kaspi, V. M., Taylor, J. H., and Ryba, M. F., "High-Precision Timing of Millisecond Pulsars. III: Long-Term Monitoring of PSRs B1855+09 and B1937+21," *Astrophysical Journal*, Vol. 428, 1994, pp. 713-728.

[6] Matsakis, D. N., Taylor, J. H., and Eubanks, T. M., "A Statistic for Describing Pulsar and Clock Stabilities," *Astronomy and Astrophysics*, Vol. 326, 1997, pp. 924-928.

[7] Detweiler, S., "Pulsar Timing Measurements And The Search For Gravitational Wave," *The Astrophysical Journal*, Vol. 234, 1979, pp. 1100-1104.

[8] Hellings, R. W., and Downs, G. S., "Upper Limits On The Isotropic Gravitational Radiation Background From Pulsar Timing Analysis," *The Astrophysical Journal*, Vol. 265, 1983, pp. L39-L42.

[9] Lommen, A. N., and Backer, D. C., "Using Pulsars To Detect Massive Black Hole Binaries Via Gravitational Radiation: Sagittarius A* And Nearby Galaxies," *The Astrophysical Journal*, Vol. 562, 2001, pp. 297-302.

[10] Sala, J., Urruela, A., Villares, X., Estalella, R., and Paredes, J. M., "Feasibility Study for a Spacecraft Navigation System relying on Pulsar Timing Information," European Space Agency Advanced Concepts Team ARIADNA Study 03/4202, 23 June 2004.

[11] Sheikh, S. I., "The Use of Variable Celestial X-ray Sources for Spacecraft Navigation," Ph.D. Dissertation, University of Maryland, 2005, URL: https://drum.umd.edu/dspace/handle/1903/2856.

[12] Sheikh, S. I., Pines, D. J., Wood, K. S., Ray, P. S., Lovellette, M. N., and Wolff, M. T., "Spacecraft Navigation Using X-ray Pulsars," *Journal of Guidance, Control, and Dynamics*, Vol. 29, No. 1, 2006.

[13] Murray, C. A., *Vectorial Astrometry*, Adam Hilger Ltd, Bristol UK, 1983.

[14] Hellings, R. W., "Relativistic Effects in Astronomical Timing Measurements," *Astronomical Journal*, Vol. 91, 1986, pp. 650-659.

[15] Backer, D. C., and Hellings, R. W., "Pulsar Timing and General Relativity," *Annual Review of Astronomy and Astrophysics*, Vol. 24, 1986, pp. 537-575.

[16] Taylor, J. H., "Pulsar Timing and Relativistic Gravity," *Philosophical Transactions of the Royal Society of London*, Vol. 341, 1992, pp. 117-134.

[17] Blandford, R., and Teukolsky, S. A., "Arrival-Time Analysis for a Pulsar in a Binary System," *Astrophysical Journal*, Vol. 205, 1976, pp. 580-591.

[18] Taylor, J. H., Manchester, R., and Nice, D. J., "TEMPO Software Package," [online], URL: http://pulsar.princeton.edu/tempo/ [cited 10 November 2002].

[19] Thomas, J. B., "Reformulation of the Relativistic Conversion Between Coordinate Time and Atomic Time," *Astronomical Journal*, Vol. 80, No. 5, 1975, pp. 405-411.

[20] Moyer, T. D., "Transformation from Proper Time on Earth to Coordinate Time in Solar System Barycentric Space-Time Frame of Reference - Part One," *Celestial Mechanics*, Vol. 23, 1981, pp. 33-56.

[21] Moyer, T. D., "Transformation from Proper Time on Earth to Coordinate Time in Solar System Barycentric Space-Time Frame of Reference - Part Two," *Celestial Mechanics*, Vol. 23, 1981, pp. 57-68.

[22] Parkinson, B. W., and Spilker, J. J. J. Eds., *Global Positioning System: Theory and Applications, Volume I*. American Institute of Aeronautics and Astronautics, Washington, DC, 1996.

[23] Martin, C. F., Torrence, M. H., and Misner, C. W., "Relativistic Effects on an Earth-Orbiting Satellite in the Barycenter Coordinate System," *Journal of Geophysical Research*, Vol. 90, No. B11, 1985, pp. 9403-9410.

[24] Seidelmann, P. K., *Explanatory Supplement to the Astronomical Almanac*, University Science Books, Sausalito CA, 1992.

[25] Richter, G. W., and Matzner, R. A., "Second-order contributions to gravitational deflection of light in the parameterized post-Newtonian formalism," *Physical Review D*, Vol. 26, No. 6, 1982, pp. 1219-1224.

[26] Richter, G. W., and Matzner, R. A., "Second-order contributions to gravitational deflection of light in the parameterized post-Newtonian formalism. II. Photon orbits and deflections in three dimensions," *Physical Review D*, Vol. 26, No. 10, 1982, pp. 2549-2556.

[27] Richter, G. W., and Matzner, R. A., "Second-order contributions to relativistic time delay in the parameterized post-Newtonian formalism," *Physical Review D*, Vol. 28, No. 12, 1983, pp. 3007-3012.

[28] Nelson, R. A., "Relativistic Effects in Satellite Time and Frequency Transfer and Dissemination," *ITU Handbook on Satellite Time and Frequency Transfer and Dissemination*, International Telecommunication Union, Geneva, (to be published), pp. 1-30.

[29] Weinberg, S., *Gravitation and Cosmology: Principles and Applications of the General Theory of Relativity*, John Wiley and Sons, New York, 1972.

[30] Richter, G. W., and Matzner, R. A., "Gravitational deflection of light at 1 1/2 PPN order," *Astrophysics and Space Science*, Vol. 79, 1981, pp. 119-127.

[31] Shapiro, I. I., "Fourth Test of General Relativity," *Physical Review Letters*, Vol. 13, No. 26, 1964, pp. 789-791.

[32] Rawley, L. A., Taylor, J. H., and Davis, M. M., "Fundamental Astrometry and Millisecond Pulsars," *Astrophysical Journal*, Vol. 326, 1988, pp. 947-953.

[33] Taylor, J. H., and Weisberg, J. M., "Further Experimental Tests of Relativistic Gravity Using the Binary Pulsar PSR 1913+16," *Astrophysical Journal*, Vol. 345, 1989, pp. 434-450.

[34] Bell, J. F., "Radio Pulsar Timing," *Advances in Space Research*, Vol. 21, No. 1/2, 1998, pp. 137-147.

[35] Lorimer, D. R., "Binary and Millisecond Pulsars at the New Millennium," *Living Reviews in Relativity*, Vol. 4, 2001, pg. 5.

[36] Epstein, R., "The binary pulsar - Post-Newtonian timing effects," *Astrophysical Journal*, Vol. 216, 1977, pp. 92-100.

[37] Haugan, M. P., "Post-Newtonian arrival-time analysis for a pulsar in a binary system," *Astrophysical Journal*, Vol. 296, 1985, pp. 1-12.

[38] Sheikh, S. I., and Pines, D. J., "Recursive Estimation of Spacecraft Position Using X-ray Pulsar Time of Arrival Measurements," *ION 61st Annual Meeting*, Institute of Navigation, Boston MA, 27-29 June 2005.

[39] NASA HEASARC, "HEAsoft: NASA's HEASARC Software," [online], URL: http://heasarc.gsfc.nasa.gov/docs/software/lheasoft/ [cited 23 May 2003].

[40] Markwardt, C., "How to read the JPL Ephemeris and Perform Barycentering," [online], 2001, URL: http://lheawww.gsfc.nasa.gov/users/craigm/bary/ [cited 23 May 2003].

[41] Possenti, A., Cerutti, R., Colpi, M., and Mereghetti, S., "Re-examining the X-ray versus spin-down luminosity correlation of rotation powered pulsars," *Astronomy and Astrophysics*, Vol. 387, 2002, pp. 993-1002.

[42] Becker, W., and Trümper, J., "The X-ray luminosity of rotation-powered neutron stars," *Astronomy and Astrophysics*, Vol. 326, 1997, pp. 682-691.

[43] Caraveo, P. A., and Mignani, R. P., "A new HST measurement of the Crab Pulsar proper motion," *Astronomy and Astrophysics*, Vol. 344, 1999, pp. 367-370.

[44] Princeton, "Princeton University Pulsar Group Pulsar Catalog," [online database], Princeton University, URL: http://pulsar.princeton.edu/pulsar/catalog.shtml [cited 4 May 2003].

[45] Nicastro, L., Cusumano, G., Löhmer, O., Kramer, M., Kuiper, L., Hermsen, W., Mineo, T., and Becker, W., "BeppoSAX Observation of PSR B1937+21," *Astronomy and Astrophysics*, Vol. 413, 2004, pp. 1065-1072.

[46] Standish, E. M., "NASA JPL Planetary and Lunar Ephemerides," [online database], NASA, URL: http://ssd.jpl.nasa.gov/eph_info.html [cited 1 December 2004].

[47] Hobbs, G. B., Edwards, R. T., and Manchester, R. N., "TEMPO2, a new pulsar-timing package - I. An overview," *Monthly Notices of the Royal Astronomical Society*, Vol. 369, 2006, pp. 655-672.

[48] Edwards, R. T., Hobbs, G. B., and Manchester, R. N., "TEMPO2, a new pulsar timing package - II. The timing model and precision estimates," *Monthly Notices of the Royal Astronomical Society*, Vol. 372, 2006, pp. 1549-1574.